

# We are IntechOpen, the world's leading publisher of Open Access books Built by scientists, for scientists

6,900

Open access books available

185,000

International authors and editors

200M

Downloads

Our authors are among the

154

Countries delivered to

TOP 1%

most cited scientists

12.2%

Contributors from top 500 universities



WEB OF SCIENCE™

Selection of our books indexed in the Book Citation Index  
in Web of Science™ Core Collection (BKCI)

Interested in publishing with us?  
Contact [book.department@intechopen.com](mailto:book.department@intechopen.com)

Numbers displayed above are based on latest data collected.  
For more information visit [www.intechopen.com](http://www.intechopen.com)



---

# The Guidelines of Material Design and Process Control on Hybrid Fiber Metal Laminate for Aircraft Structures

---

Sang Yoon Park and Won Jong Choi

Additional information is available at the end of the chapter

<http://dx.doi.org/10.5772/intechopen.78217>

---

## Abstract

Fiber metal laminate (FML) is a hybrid material system that consists of thin metal sheets bonded into a laminate with intermediate thin fiber reinforced composite layers. The aerospace industry has recently increased their use of FMLs due to the considerable weight reduction and consequent benefits for critical load-carrying locations in commercial aircraft, such as upper fuselage skin panels. All FML materials and their processes should be qualified through enough tests and fabrication trials to demonstrate reproducible and reliable design criteria. In particular, proper surface treatment technologies are prerequisite for achieving long-term service capability through the adhesive bonding process. This chapter introduces a brief overview of design concept, material properties and process control methodologies to provide detailed background information with engineering practices and to help ensure stringent quality controls and substantiation of structure integrity. The guidelines and information found in this chapter are meant to be a documentation of current knowledge and an application of sound engineering principles to the FML part development for aerospace usage.

**Keywords:** fiber metal laminate (FML), mechanical behaviors, surface treatment, process control, long-term durability


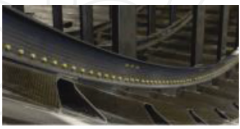

---

## 1. Introduction: choice of materials in aircraft design

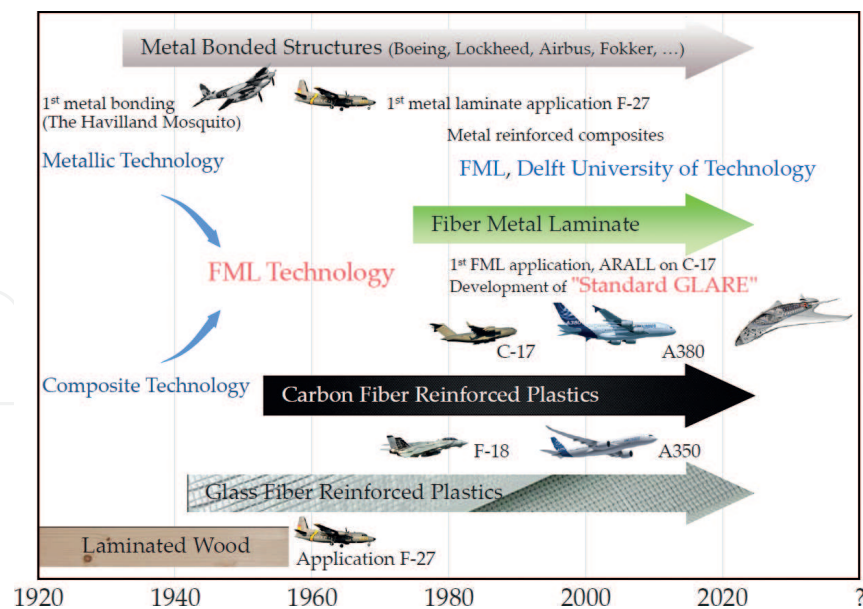
The current trends in commercial aircraft operations are showing an increasing demand for lower operational and maintenance costs. The maintenance costs, directly incurred by the airlines' operation, are an important measure of the economic benefits associated with reducing direct operating cost [1]. Practically, most aircraft structures are being designed for longer design lifetime with extension of inspection intervals. For this purpose, the fatigue and

damage tolerance (F&DT) properties have been received considerable attention for further use of lightweight materials on next generation aircrafts [2]. Therefore, there is a strong need for the application of more durable and damage tolerant materials to minimize the total maintenance costs of commercial aircraft. Reducing the structural weight can lead to better fuel efficiency, reduced CO<sub>2</sub> emissions and lower maintenance costs. Nowadays, two competing materials, such as modern aluminum alloys and composites, have the potential to improve the cost effectiveness, but they still have limitations that restrict their widespread use, for example corrosion-fatigue resistance for aluminum alloys and blunt notch strength and impact resistance for carbon fiber reinforced plastics (CFRP) [3]. The basic characteristics of materials for aircraft structures are given in **Table 1**.

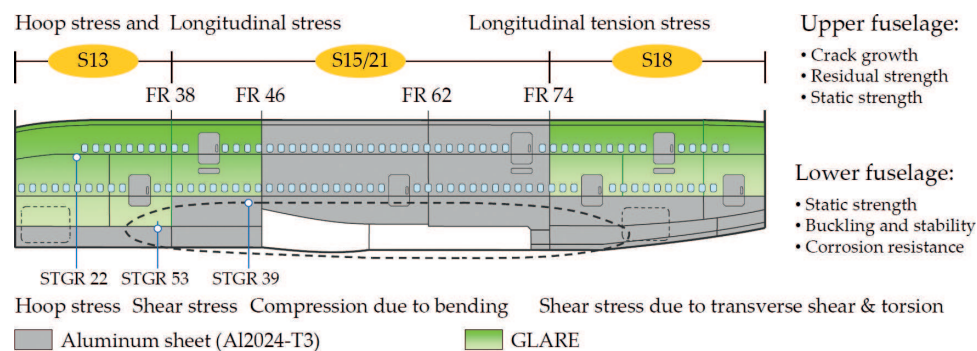
A chronological history of materials for aircraft structures is illustrated in **Figure 1**. New multi-layered hybrid materials, FMLs consist of thin metal sheets bonded into a laminate with intermediate thin fiber reinforced composite layers, and combines the benefits of both material classes [5]. Recently, the use of FMLs leads to subsequent benefits for primary aircraft structures, for example upper fuselage skin panels as shown in **Figure 2** [6–8]. This figure also presents typical load cases for dimensioning criteria in the design of fuselage structures. To date, the representative commercially available FML is glass reinforced aluminum laminate (GLARE), which combines thin aluminum sheets with unidirectional glass fiber reinforced epoxy layers [9, 10]. It has been produced for the upper fuselage skin panels of Airbus A380 (Toulouse, France) at GKN Aerospace’s Fokker Technologies (Papendrecht, The Netherlands) in collaboration with AkzoNobel (Amsterdam, The Netherlands) and Alcoa (New York, US) [3, 4, 11]. The FMLs are also being considered for thin-walled structures for single aisle fuselage shells. In addition, their superior F&DT properties which are addressed as essential design principles in JAR/FAR 25.571 (Damage-tolerance and fatigue evaluation of structure) make them the ideal candidate for military aircrafts that such applications are not only subject to high fatigue stresses, but also high-velocity impact damages (e.g. battle damages) [12]. Concurrently, other types of commercially available FMLs are aramid aluminum laminate (ARALL) based on aramid fibers and carbon reinforced aluminum laminate (CARALL) based on carbon fibers, respectively [11].

Materials	Aluminum alloys	Composites (CFRP)	FML
			
Strength	<ul style="list-style-type: none"> <li>Broad experience</li> <li>Repairability</li> <li>Static behaviors</li> <li>Improvement potential</li> </ul>	<ul style="list-style-type: none"> <li>Fatigue behaviors</li> <li>Low density (1.54 g/cm<sup>3</sup>)</li> <li>No corrosion</li> <li>Best suited for smart structures</li> </ul>	<ul style="list-style-type: none"> <li>Improved fatigue</li> <li>Better tailoring</li> <li>Higher fire resistance</li> <li>Less corrosion</li> </ul>
Weakness	<ul style="list-style-type: none"> <li>High density (2.78 g/cm<sup>3</sup>)</li> <li>Fatigue behaviors</li> <li>Corrosion behaviors</li> <li>High costs of new alloys</li> </ul>	<ul style="list-style-type: none"> <li>Poor impact behaviors</li> <li>No plasticity</li> <li>Repairability</li> <li>Recycling</li> </ul>	<ul style="list-style-type: none"> <li>Lower stiffness</li> <li>Higher density (2.52 g/cm<sup>3</sup>)</li> <li>Less industrialized process (compared to CFRP)</li> </ul>

**Table 1.** Strength and weakness of materials for aircraft structures [4].



**Figure 1.** Chronological history of materials for aircraft structures (reproduced from Fontain [3]).



**Figure 2.** GLARE application on Airbus A380 fuselage section-13/18: Total GLARE area is 469 m<sup>2</sup>, 27 panels (reproduced from Beumler [4]) and typical load cases on GLARE sections (reproduced from Assler and Telgkamp [13]).

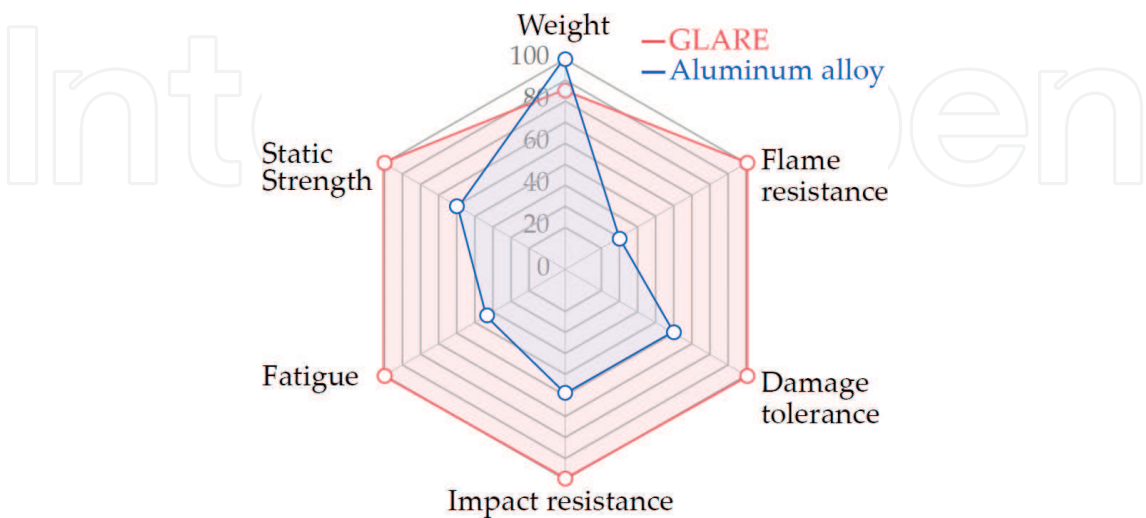
The first generation FML, the ARALL, was introduced at 1978 in Faculty of Aerospace Engineering at TU Delft (Delft University of Technology, The Netherlands) [14]. The ARALL consists of alternating thin aluminum alloy layers (0.2–0.4 mm) and uniaxial or biaxial aramid fibers. The GLARE which is the second generation of FML presents the excellent fatigue resistance with high blunt notch strength than either 2024-T3 or ARALL. This new hybrid material also offers the actual weight reduction when it is applied to the fuselage skin panels [15, 16]. Finally, a much stiffer FML which is made by carbon fiber instead of aramid and glass fibers, the CARALL, had been also investigated in TU Delft [17]. The use of high modulus of carbon fiber (in typical, ranging from 230 to 294 GPa) exhibits more efficient crack bridging at the preliminary stage of fatigue crack propagation within composite layers [18]. However, the residual strength of notched CARLL is significantly lower than the monolithic aluminum alloys due to the limited failure strain of carbon fiber (in typical, 2.0%) [11]. Furthermore, it is more susceptible to galvanic corrosion when aluminum alloys are electrically connected to carbon fiber reinforced composites [19–21].

## 2. Material property behaviors of GLAREs

### 2.1. Mechanical behaviors of GLAREs for aircraft structures

GLAREs boast a large number of favorable characteristics, such as low density, static strength, better F&DT properties, high impact and flame resistances, as shown in **Figure 3** [22–24]. More descriptions on advantages of GLAREs are provided as follows:

- *Lightweight:* High static strength of GLARE2 in 0° fiber direction contributes to weight saving over the aluminum alloys by roughly 6% in the design based on bending stiffness, and by 17% in the design based on yield strength, respectively [25]. For example, the use of GLAREs on A380 fuselage shells achieves a weight saving of up to 794 kg (−10%) compared with the aluminum alloys [26]. The typical density of standard GLAREs is the range from 2.38 to 2.52 g/cm<sup>3</sup>.
- *High strength:* It is apparent that the GLAREs reinforced with unidirectional glass fiber have anisotropic properties. This glass fiber contributes to increase in static strength and elastic modulus in the longitudinal direction along which the glass fiber is oriented. On the other hands, the aluminum sheets control overall mechanical properties of GLAREs in the transverse direction. As a result, the unidirectional GLAREs (e.g. GLARE1 and GLARE2) exhibit the high ultimate tensile strength compared with the aluminum alloys in the longitudinal direction, and it contributes to weight reduction in the case of tension-dominated structural components. In contrast, the transverse strength is somewhat lower than those of aluminum alloys. To overcome this limitation, the cross-ply GLAREs (e.g. GLARE3 and GLARE5) and angle-ply GLARE (e.g. GLARE6) have been introduced to provide the balanced mechanical properties in both directions [26].
- *High fatigue resistance:* The superior fatigue resistance is a result of fiber bridging mechanism whereby the intact fiber layers provide an alternative load path around the cracked metal layers, eventually reducing local stress in front of crack tip [27]. Vogelesang et al.

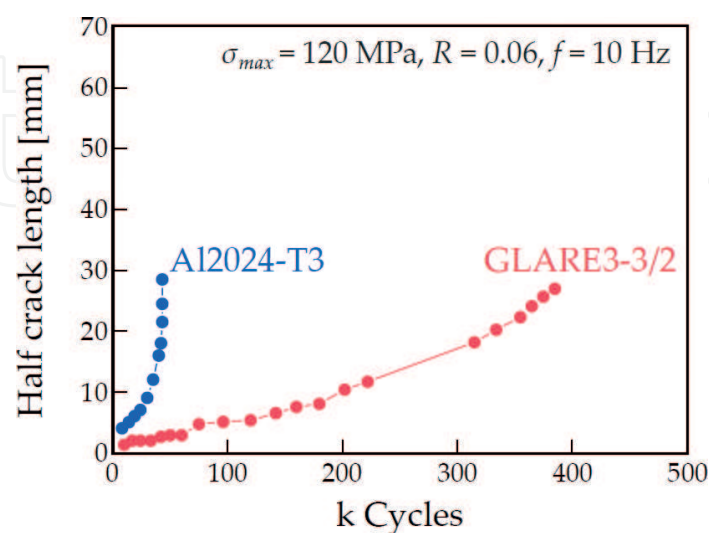


**Figure 3.** GLARE vs. aluminum alloy comparison ratio.

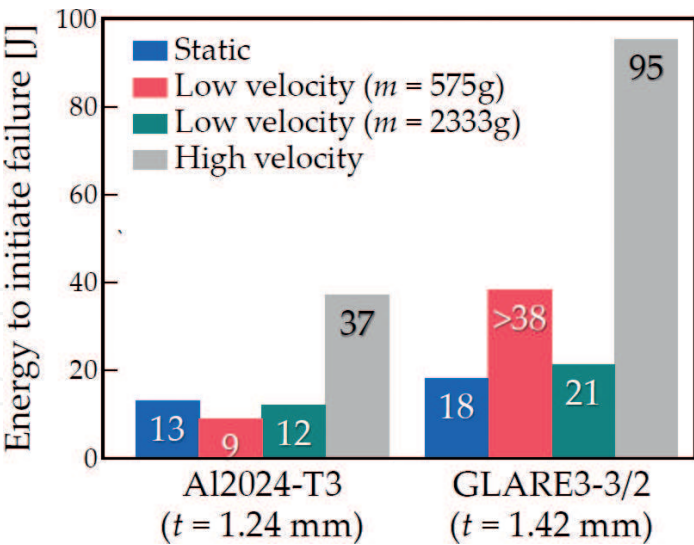


[28] reported that GLARE3-3/2 exhibit almost constant slow crack-growth when it is subjected to constant-amplitude fatigue loading as shown in **Figure 4**. Such low fatigue crack growth rate can lead to the minimal scheduled inspection downtime of aircraft.

- *Blunt notch strength*: The notched residual strength is also an important design parameter since the geometrical notches (e.g. cutouts to serve as doors and windows) are inevitable in the design of fuselage shells. Although the GLARE presents a relatively high notch sensitivity compared with ductile aluminum alloys, and the use of high ultimate strength S2-unidirectional glass fiber (in typical, 4890 MPa) makes it superior to ARALL in notch strength [26]. Hagenbeek et al. [29] proposed a numerical simulation model for predicting blunt notch strength by considering the metal volume fraction based on Norris failure criterion, and they reported that such approach has been shown to be effective for use in predicting multi-axial blunt notch strengths (i.e. biaxial and shear components) of GLARE.
- *High impact resistance*: Impact resistance is actually a significant advantage of GLARE, especially when compared to either aluminum alloys or CFRP [30]; **Figure 5** compares the respective impact energy absorbing capacities based on the through-the-thickness cracking (i.e. puncture energy). Obviously, GLARE3-3/2 shows higher impact resistance to cracking than aluminum alloy. This result may be attributed due to the localized fiber fracture and the extensive shear failure in the outer aluminum sheets [31, 32]. In addition, a high strain rate strengthening phenomenon which occurs in the glass fibers, combined with their relatively high failure strain contribute to increase in the impact resistance of GLARE, rather than other FMLs, such as ARALL and CARALL [33].
- *Burn-through capabilities*: To meet the airworthiness standard of a max. 90 seconds evacuation time (JAR/FAR 25.803: Emergency evacuation), a structural integrity of fuselage is of major importance in order to prolong a safe environment of the passengers in the event of a post-crash fire scenario. Apparently, the GLARE shows high thermal insulation



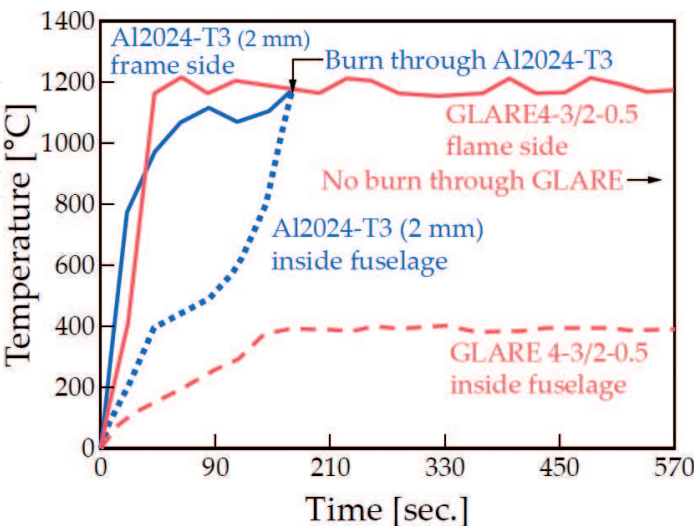
**Figure 4.** Fatigue crack growth [14].



**Figure 5.** Comparison of low-velocity impact performance [15].

performance, and subsequently contributes to enhancing structural integrity in fuselage shells as shown in **Figure 6**. Owing to high melting temperature of S2 glass fiber (in typical, 1466°C), only the outer aluminum sheet starts to melt and separates from the other layers. As a result, the unexposed side of GLARE panel would remain relatively intact where the unexposed side temperature was just below 400°C.

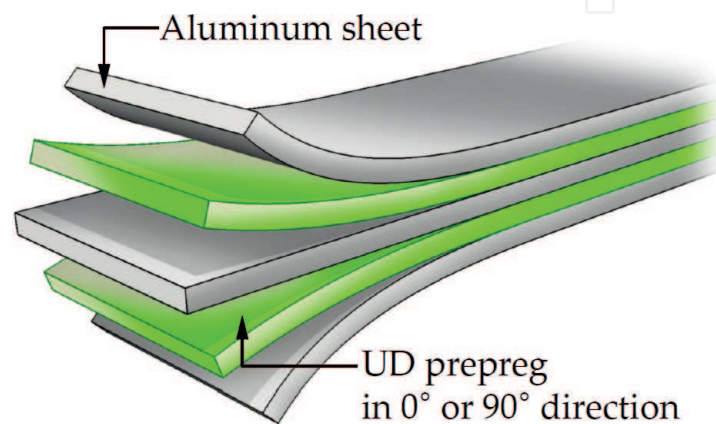
- Long-term hygrothermal behaviors:** In general, the significant changes in moisture absorption are not observed by GLAREs, which confirmed well to the shielding effect of the outer aluminum sheet in this material [35, 36]. However, in the case of thermal cycling exposure, the decrease rate of GLAREs is 1–7% higher than those of glass fiber-reinforced composites. This reduction is attributed to the large coefficient of thermal expansion (CTE) difference between their constituent materials [35].



**Figure 6.** GLARE fire resistance comparing to aluminum alloy [34].

## 2.2. GLARE grades

Another beneficial feature of GLARE is that the number and orientation of composite layers can be selected to best suit different applications, and such material features make it attractive for structural applications [37]. For the certification of GLAREs for aircraft structures, several lay-up patterns are already defined as a standard grade: the schematic view of GLARE 3/2 is shown in **Figure 7**. This approach is useful to define the specific lay-up pattern used in the structural design [38]. Nowadays, the standard GLAREs are being produced in six different grades as listed in **Table 2** [39]. All grades are classified according to the type of lay-up pattern where the composite layers consists of unidirectional S2 glass fiber (AGY Holding Corp., USA)



**Figure 7.** Schematic view of GLARE 3/2.

Grade	Metal layers		Prepreg layers		Typical density (g/cm <sup>3</sup> )	Characteristics
	Grade	Thickness (mm)	Orientation	Thickness (mm)		
GLARE1	7475-T761	0.3–0.4	0/0	0.25	2.52	<ul style="list-style-type: none"> <li>Unidirectional loaded parts with rolling direction aluminum sheet in loading direction (stiffeners)</li> </ul>
GLARE2	2024-T3	0.2–0.5	0/0	0.25		
	2024-T3	0.2–0.5	90/90	0.25		
GLARE3	2024-T3	0.2–0.5	0/90	0.25	2.52	<ul style="list-style-type: none"> <li>Bi-axially loaded parts with 1:1 of principle stresses (fuselage skins, bulkheads)</li> </ul>
GLARE4	2024-T3	0.2–0.5	0/90/0	0.375	2.52	<ul style="list-style-type: none"> <li>Bi-axially loaded parts with 2:1 of principle stresses with aluminum sheet in main or perpendicular loading direction (fuselage skins)</li> </ul>
	2024-T3	0.2–0.5	90/0/90	0.375		
GLARE5	2024-T3	0.2–0.5	0/90/90/0	0.5	2.38	<ul style="list-style-type: none"> <li>Impact critical areas (floors &amp; cargo liners)</li> </ul>
GLARE6	2024-T3	0.2–0.5	–45/+45	0.5	2.52	<ul style="list-style-type: none"> <li>Shear, off-axis properties</li> </ul>

(a) The number of orientations is equal to the number of unidirectional prepreg ply in each composite layer. The thickness in mm corresponds to the total thickness of composite layers in between two aluminum layers.  
(b) The rolling direction (axial) is defined as 0°, and the transverse rolling direction is defined as 90°.

**Table 2.** Classification of GLARE for aircraft structures [5, 12, 39].



and FM<sup>®</sup>94 modified epoxy (Cytec-Solvay Group, USA). Nominal fiber volume fraction and ply thickness of prepreg are 59% and 0.125 mm, respectively [39].

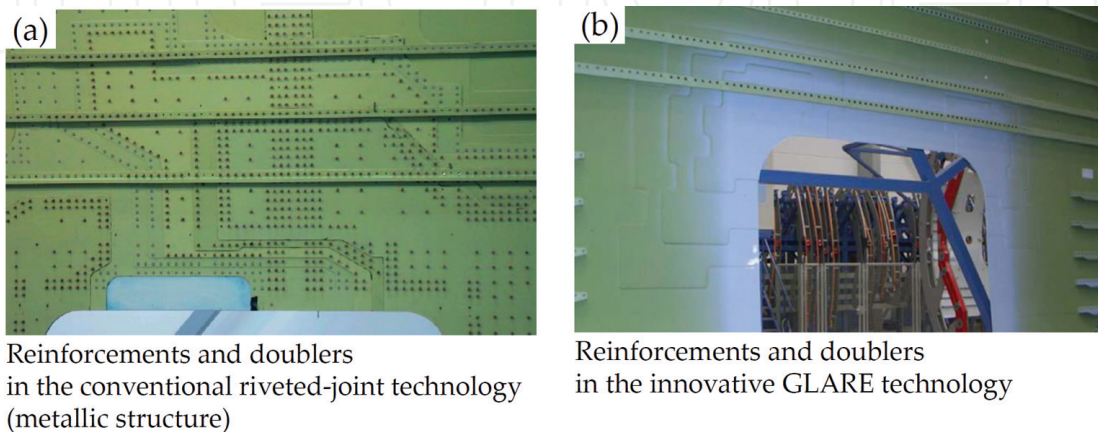
A special coding convention is used to describe the different GLARE grades and specify their lay-up patterns. Symbolically, a general configuration is represented as follows [5]:

$$\text{GLARE } N_G = N_{al}/N_{gl} - t_{al} \quad (1)$$

where;  $N_G$  is the number indicating GLARE grade,  $N_{al}$  is the number of aluminum layers,  $N_{gl}$  is the number of composite layers ( $N_{gl} = N_{al} - 1$ ) and  $t_{al}$  is the thickness of each separate aluminum sheet (in typical, 0.25–0.5 mm). Each composite layer in turn consists of a certain number of unidirectional prepreg plies in  $0^\circ/90^\circ/\pm 45^\circ$  directions. For example, each composite layer in GLARE4 consists of two unidirectional prepreg plies in oriented at  $0$  and  $90^\circ$  with respect to the rolling direction of aluminum sheets. Thereafter, GLARE4B-3/2 comprises three cross-pplies within a composite layer, for example two layers in  $90^\circ$  and one layer in  $0^\circ$  direction. The fraction of unidirectional fibers in the rolling direction is twice much than that in the perpendicular direction.

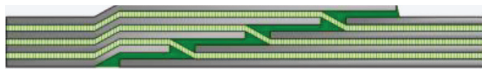
### 2.3. Design philosophy for GLARE structures

An introduction of new materials for aircraft structures took place in evolution steps which suggests a realistic application of the innovative design philosophy, eventually leading to optimization of design concept. The innovative design concept of GLAREs on A380 fuselage shells is shown in **Figure 8** [40]. The structural efficiencies, such as damage tolerance and residual notch strength are much better served by incorporating the local variations in skin panel thickness with adhesively bonded joints. In early stage of technology development, GLARE structures were produced only as a flat panel. The innovations in structural design have been developed to overcome the joining problem and is termed the splice joint. The first splice concept consisted of butted aluminum sheets with the composite layer bridging the splices (e.g. butt joint). However, this concept is not recommended for structural applications because of premature failure in the butts. To overcome this limitation, several designs of splice concepts where two aluminum sheets are positioned with a slight over-lap forming a single metal sheet layer are introduced, as shown in **Table 3** [41].



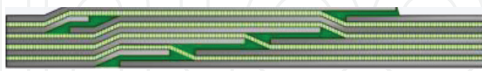
**Figure 8.** Construction and production possibility with the optimized GLARE panel (reproduced from Wischmann [40]).

Splice in skin panel or doublers



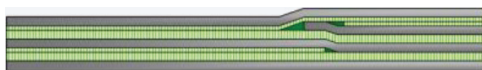
- Lamination of aluminum sheet width
- Internal stress level in double curved panels

Inter-laminar doublers



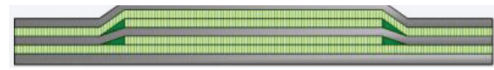
- Spliced, go through depending on length/orientation

Transition of GLARE type



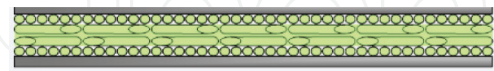
- e.g. GLARE4 to GLARE3

Additional glass fiber layers



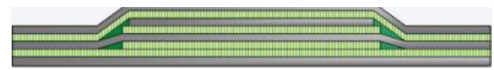
- Embedded at frame locations

Fiber oriented and lay-up



- Adjust properties to loading condition

Additional layers:



- Aluminum sheet locally at frame station
- Glass layers locally between two aluminum sheets

**Table 3.** GLARE design features–“giant tool box” (reproduced from Pleitner [41]).

For example, alternating layers (i.e. aluminum sheets and unidirectional S2 glass/epoxy prepreg plies) are laid up over the curing tool, in which forms single, or double curvature shape [5, 42]. The splices are then staggered with respect to each other, while the adhesive layers are continuous. This interlaminar doubler solution can offer the local thickness variations in the skin panel [43]. Furthermore, this design concept can allow tailor-made skin panels of any size, not limited by the standard width of aluminum sheet rolls (in typical, 1.5 m). Now, the practical limitation of panel sized is only defined by autoclave size. The thickness variations in the skin panel are generally utilized for compliance with the fail-safe design requirements and the cost-effective part production for integrating the fuselage structures between skin panels, longitudinal stringers and circumstance frames. However, the difficulties in the production of splice GLARE panels in two bonding cycles demand for a feasible production solution, which allows for completing a splice joint including doublers through co-curing process. For this purpose, a SFT (Self-Forming Technique) can provide a smart solution to produce the required doublers without an additional cure cycle for bonding the doublers over the base GLARE panel. Such an inter-laminar panel highlights the advantages of using a SFT process as follows: (1) no dimensional tolerance issue for overlap in double curvature panel, (2) the evacuation of entrapped air or volatiles in composite layers through splice (adhesive squeeze-out). It therefore allows for the increased fuselage panels width with reducing the additional joints, structural weight and production cost [5].

## 2.4. Metal volume fraction (MVF)

For the standard GLARE grades qualified, their in-plane static properties can be defined by simple prediction based on MVF, which can reduce the additional experimental testing for material qualification. A terminology, MVF, reflects the relative contribution of aluminums

properties to the properties of GLARE [5]. As a result, the MVF approach is useful for the prediction of static strength properties for GLARE as found in the literatures [5, 44, 45]. The MVF value can be calculated as follows:

$$MVF = \sum_{p_{metal}}^t t_{al} / t_{laminate} \quad (2)$$

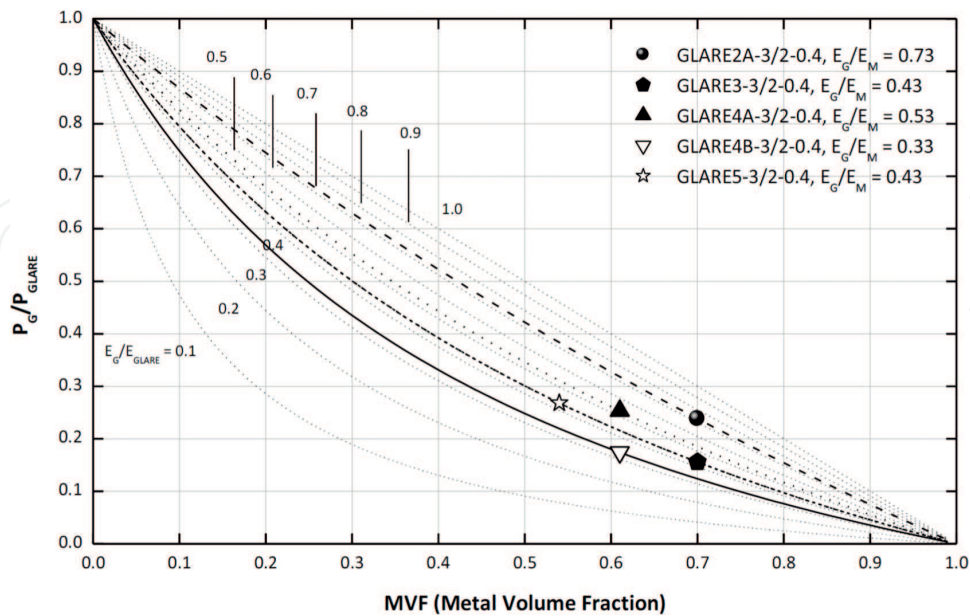
where;  $t_{al}$  is the thickness of each separate aluminum sheet,  $t_{laminate}$  is the total thickness of GLARE panel and  $p_{metal}$  is the number of aluminum sheets [5]. The typical MVF values of the standard GLARE grades are valid in a range between 0.55 and 0.70. The material property of GLARE having any MVF can be calculated by using a linear relation which follows the “rule of mixtures” available in anisotropic mechanics by using the Eq. (3).

$$E_{GLARE} = E_M \cdot MVF + E_G(1 - MVF) \quad (3)$$

where;  $E_{GLARE}$  is the elasticity of GLARE and  $E_M$  and  $E_G$  are the elasticity of aluminum sheet and composite layers, respectively. The load transfer ratio for composite layers ( $P_G/P_{GLARE}$ ) in GLARE according to MVF can be defined as follows:

$$\frac{P_G}{P_{GLARE}} = \frac{E_G/E_M}{E_G/E_M + MVF/(1 - MVF)} \quad (4)$$

The load transfer ratio for composite layers in GLARE according to MVF can be predicted as shown in **Figure 9**. It is worth noting that the load transfer ratio of composite layer in GLARE exponentially decreases with the fraction of aluminum sheets. As the fraction of aluminum sheets in GLARE decreases, more shear load can be dissipated through the aluminum sheet-composite interface [6].



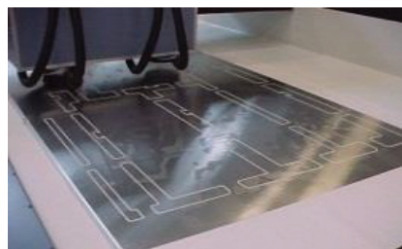
**Figure 9.** Plot of load transfer ratio for glass/epoxy layers in GLARE according to MVF for various modulus ratios of  $E_G/E_M$ : The corresponding GLARE grades of • GLARE2A 3/2–0.4 (0.703), ◆ GLARE3 3/2–0.4 (0.703), ▲ GLARE4A 3/2–0.4 (0.612), ▽ GLARE4B 3/2–0.4 (0.612) and ☆ GLARE5 3/2–0.4 (0.542).

### 3. Process control methodologies for producing GLARE structures

#### 3.1. Part production and quality controls

Basically, the production process for making GLARE structures is similar to the traditional production of metallic bonded structures and composite laminates. Before the parts are released, the part's quality should be assured through a reliable quality control (QC) method. For this purpose, the stringent QC procedures shall be developed and applied to the part production of GLAREs. At this time, the QC system includes all procedures that ensure the raw material quality, in-process control monitoring and verification of fitness for part acceptance. At each production stage, the key process parameters should be also standardized with the specified production tolerances as the follows [4, 5, 41]:

- *QC of raw materials.* GLARE manufacturer starts with the preparation with rolls of thin aluminum bare sheet (in typical, 0.3–0.4 mm). A custom-built machine decoils the thin aluminum sheet from rolls, and flattens the sheet and cuts it to lengths of up to 11 m for large skin panels. Next, the cut sheets are milled in accordance with the engineering drawings. At this time, all the aluminum sheets and unidirectional prepreg plies should be controlled by raw materials inspection specifications, and some specific properties should be controlled: (1) rolling direction, straightness, waviness and surface roughness for aluminum sheets; (2) fiber direction, prepreg bridging, or wrinkles and shelf-life requirements (e.g. storage life and mechanical life) for prepreg plies. This QC activity is basically the same as the traditional production of sheet metal forming, or composites. All prepreg shall be cut over a clean, non-contaminated surface with clean, sharp knives, or digital cutting machine to minimize distortion and splitting. The pre-cut materials (i.e. kit) should be stored in flat or stress-free condition to prevent folding or further damage. Unless otherwise specified by the engineering drawings, all the prepreg size should have a suitable trim at required locations to keep irregular edges out of the final part dimension.



[Source: CompositesWorld]



- *QC of surface treatment.* Surface of aluminum bare sheet should be pre-treated to obtain a proper adhesion strength and durability with the prepreg resin. For this purpose, the milled sheets are transferred via a handling system to the chemical treatment line. The standard surface treatment process consists of solvent degreasing, CAE (Chromic-Sulfuric Acid Etching), CAA (Chromic Acid Anodizing), and followed by organic bond primer. All key process parameters should be checked for each batch of aluminum sheets according to the corresponding Airbus's own specifications, for example deoxidizing/anodic bath temperature, solution chemistry, rinse water purity and so forth. The specific surface treatment procedures of aluminum alloys are going to be explained in detail Section 3.2. Finally, the primed, cut sheets are re-rolled, and covered in a protective black plastic (or paper) bag for storage until needed in fabrication.



[Source: Fokker]

- *Control of lay-up process.* Alternating layers of aluminum bare sheets and prepreg plies are positioned in the right stacking order in accordance with GLARE grade. All the lay-up works should be conducted in a sufficiently clean environment, and the working environment such as temperature and humidity should be also kept below well-defined levels. All cut prepreg plies should be sequentially prepared and collated on the curing tool in the location and orientation as per the engineering drawings, or shop process instruction. An optical LPS (Laser Projection System, Virtek Vision International Inc., Waterloo, ON, Canada) may be capable of attaining the required dimension tolerance.



[Source: Fokker]



- *Control of autoclave process.* The laid-up parts are vacuum bagged, and then placed into the autoclave to be united by heat and pressure. Autoclave facility shall have instrumentation which autographically records time, temperature, pressure and vacuum where applicable. All gauges shall be controlled and periodically calibrated and certified in accordance with the procedures approved by the QC department. During an autoclave cure cycle, a high compaction pressure (in typical, 11 bar) is normally applied to the GLARE lamination stack at an elevated curing temperature (in typical, 125°C) for 3.5 hours. The representative manufacturing-induced defects, such as voids, porosities, should be accurately controlled to prevent internal defects. In addition to the QC activities in the part production of GLARE, there is also required to perform a “final check” prior to the part release. Non-destructive inspection (e.g. ultrasonic C-scanner) and some mechanical tests are generally accomplished in the final step of QC.



[Source: CompositesWorld]

- *Post processing.* The manufacturing and assembly of GLARE structures typically require machining operations, such as milling and drilling. For examples, the GKN Aerospace's Fokker business has been produced a large-sized GLARE panel of  $4.5 \times 11.5$  m by using a 5-axis milling machine on a movable bed. However, a technique for machining of this multi-layered structure has presented more challenges in the aerospace industry than aluminum alloys or composites due to the coupled interaction between composite- and metal-phase cutting. The machining operations should be accomplished to meet the acceptance limit for the discrepancies as per the engineering drawing, or process specification.



[Source: CompositesWorld]

### 3.2. Surface treatment of aluminum alloys for producing GLARE structures

A strong bonding interface is one of the key factors for improving the durability of GLAREs. It is apparent that the surface treatment technique can improve the surface energy and wettability of metallic substrates, and is an effective method for enhancing the bonding strength between a metal substrate and a fiber reinforced polymer composite [46]. In addition, the surface treatment can remove the undesirable surface oxides or contaminants on the metallic substrate, and ameliorate the surface composition and microstructure of the metallic substrate [6, 47]. This allows the fiber bridging mechanism and mechanical properties of GLAREs to be improved, and moreover, the crack propagation rate at the aluminum-composite interface can be effectively reduced [48, 49]. Previous research works reported that the surface treatment should be carefully taken into consideration when improving interlaminar shear strength at the aluminum-composite interface [6, 50], environmental durability and low-velocity impact resistance of GLARE. Therefore, the proper production steps should be clearly defined before any production process is implemented. Note that this section is described based on our previous surface treatment studies of aluminum alloys for aircraft structures [46].

All the anodizing process are complex multi-stage operations incorporating degreasing and deoxidizing stages, as described in the preceding sections, plus appropriate rinses. Anodizing oxidation in solution of CAA or PAA is the preferred stabilizing treatment for the structural adhesive bonding of aluminum alloys in critical applications such as aircraft structures [51, 52]. However, they typically rely on such hazardous materials as strong acid and hexavalent chromium. The use of chromate is prohibited, or progressively banned in most industries due to its carcinogen activity. For this purpose, non-chromate anodizing such as boric-sulfuric acid anodizing (BSAA), or phosphoric-sulfuric anodizing (PSA), have been developed since the mid-1990s [51, 53], but neither of them have been fully validated for aircraft applications. Typical anodizing processes and their process parameters are listed in **Table 4**.

The classical porous oxide structure which are produced by anodizing process is likely to be related to capillary forces of primer trying to penetrate into the oxide pores, which in turn increase in mechanical interlocking between anodic oxide and primer [46]. The porous oxide structures can be controllable in accordance with the anodizing processes, as listed in **Table 5**. This table clearly represents the effects of anodizing processes on the oxide structures in terms of oxide thickness, pore diameter and cell wall thickness. The CAA process was found to give a relatively thick and softer oxide structure than those formed by the other processes [52]. This was established as an effective pretreatment for adhesive bonding with superior durability performance in service [51, 52, 54]. The European aerospace industry is still using this method [51, 52]. However, notwithstanding the remarkable durability data in corrosive environments, the use of chromate treatment process is being restricted due to recent environmental policy.

The PAA process is basically used for the structural adhesive bonding of aluminum and its alloys. The standard process (Boeing's BAC 5555 or ASTM D 3933) has proven to produce the most durable and reactive surface for structural adhesive bonding [57]. The PAA substrates are normally submitted to a Forest Product Laboratory (FPL) etch prior to anodizing, although the non-chromate acid etch (P2) is sometimes used instead. The PAA-treated anodic oxide is highly porous with open cell diameter of approximately 32 nm in height on top of a much

Treatments <sup>1</sup>	CAA [51]	PAA [54]	BSAA [51]	PSA [53]
Electrolyte (wt%)	2.5–3.0 (CrO <sub>3</sub> )	10 (H <sub>3</sub> PO <sub>4</sub> )	5.0–10.0 (H <sub>3</sub> BO <sub>3</sub> )/ 30.0–50.0 (H <sub>2</sub> SO <sub>4</sub> )	10.0 (H <sub>3</sub> PO <sub>4</sub> )/ 10.0 (H <sub>2</sub> SO <sub>4</sub> )
Voltage (V)	40.0 ± 1.0	10.0	15.0 ± 1.0	18 ± 2.0
Time (min)	35–45	20	18–22	15
Temperature (°C)	40.0 ± 2.0	25.0	26.7 ± 2.2	27.0 ± 2.0
Contamination controls	<ul style="list-style-type: none"><li>• Control Cl<sup>-2</sup> &amp; sulfate impurity</li><li>• Incorporation of BaCO<sub>3</sub> powder<sup>3</sup> to remove impurity</li></ul>	<ul style="list-style-type: none"><li>• Control Cl<sup>-</sup> &amp; F<sup>4</sup></li><li>• Filtering required to remove fungus</li></ul>	<ul style="list-style-type: none"><li>• Prone to biological contamination<sup>5</sup></li><li>• Use of sodium benzoate or benzoic acid to prevent fungus growth</li></ul>	<ul style="list-style-type: none"><li>• Control Cl<sup>-</sup> &amp; F</li><li>• The installation of preventive devices for fungus growth (e.g. filters and UV lamps)</li></ul>
Racks	Al, Ti, Al with Ti-tips	Equivalent to CAA	Equivalent to CAA	Equivalent to CAA
QC issues	<ul style="list-style-type: none"><li>• Appearances</li><li>• Solution chemistry</li><li>• Water purity</li><li>• Air cleanliness</li><li>• Voltages</li><li>• Bath temperature</li></ul>	<ul style="list-style-type: none"><li>• Appearances</li><li>• Solution chemistry</li><li>• Water purity</li><li>• Air cleanliness</li><li>• Voltages</li><li>• Coating weight</li></ul>	<ul style="list-style-type: none"><li>• Appearances</li><li>• Solution chemistry</li><li>• Water purity</li><li>• Air cleanliness</li><li>• Voltages</li></ul>	<ul style="list-style-type: none"><li>• Appearances</li><li>• Solution chemistry</li><li>• Water purity</li><li>• Air cleanliness</li><li>• Voltages</li></ul>

<sup>1</sup>The proprietary materials and exact production steps are slightly dissimilar between organizations.

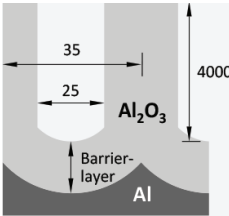
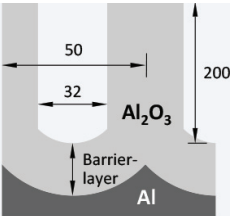
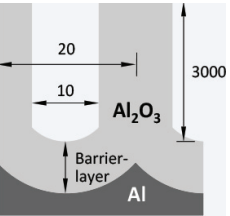
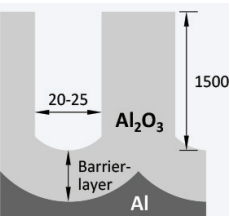
<sup>2</sup>Cl: Chloride ions.

<sup>3</sup>BaCO<sub>3</sub>: Barium carbonate.

<sup>4</sup>F: Fluorine.

<sup>5</sup>Bio-contaminant organisms, for example fungal (alternaria, fusarium and penicillium species) and bacterial (pseudomonas species).

**Table 4.** Anodizing processes for structural adhesion bonding of aluminum alloys (reproduced from Park et al. [46] with permission from Taylor & Francis).

Treatments	CAA [51]	PAA [55, 56]	BSAA [51]	PSA [53]
Oxide thickness (nm)	4000	200	3000	1500
Pore diameter (nm)	25	32	10	20–25
Cell wall thickness (nm)	10	18	10	—
Schematic view of oxide structure [nm] (non to scale)				

**Table 5.** Comparison of oxide morphology on 2024-T3 bare aluminum alloys (reproduced from Park et al. [46] with permission from Taylor & Francis).

thinner barrier layer [54, 55, 58]. The PAA oxide thickness is typically reported in the range from 200 to 400 nm with a much thinner barrier layer of about 10 nm [54, 55]. The physical comparisons between PAA and CAA oxide structures clearly represent the PAA oxide to have a much more open porous structure, which would be more easily penetrated by the subsequent organic bond primer, thereby drawing the organic polymer into the oxide structure to form a very strong interlocking interphase. The PAA oxide structure provides either equivalent or better durability results than the CAA oxide structure in the most experimental trails [59].

The BSAA process is usually carried out using a mixture of 5–10 wt.% boric acid ( $\text{H}_3\text{BO}_3$ ) and 30–50 wt.% sulfuric acid ( $\text{H}_2\text{SO}_4$ ) at  $26.7 \pm 2.2^\circ\text{C}$ . This process was patented by Boeing as a direct replacement to the CAA process [51, 60]. It is well known that the CAA process produces a chromium mist that is hazardous to health if inhaled. The BSAA is an alternative that eliminates this concern and the need for mist control. The process standard, BAC 5632, involves deoxidizing with tri-acid solutions, consisting of sodium dichromate, sulfuric, and hydrofluoric acid (HF), followed by the application of boric and sulfuric acid anodizing. The parts are then dried in warm air at  $75^\circ\text{C}$  prior to bond primer application. The anodic film which is produced by the standard BSAA has relatively small pore diameter (10 nm) compared with the conventional CAA film (25 nm), as listed in **Table 5**. The anodic oxide structure from the BSAA has a paint adhesion that is equal, or superior, to the one formed on CAA [51, 60]. For this purpose, the BSAA process parameters have been modified by the research groups, for example [61]. As a result, the required surface topography and equivalent mechanical stability in strength and durability are only enhanced when the following process variations were instituted: electrolytic phosphoric acid deoxidizer (EPAD) [51]; anodizing bath temperature in the BSAA bath [51, 61] and additional post treatment using a PAD [51].



More recently, a variety of alternative chromate-free electrochemical treatments have been introduced in the context of corrosion protection and adhesive bonding of aluminum and its alloys. The new eco-efficient alternatives developed by Airbus include tartaric-sulfuric acid anodizing (TSA) and PSA. In particular, a significant step towards chromate-free has been achieved by PSA process for adhesively bonded joints. This process, which is utilized for adhesive bonded joints is usually carried out by using a mixture of 10 wt.% phosphoric acid ( $\text{H}_3\text{PO}_4$ ) and 10 wt.% sulfuric acid ( $\text{H}_2\text{SO}_4$ ) at temperatures ranging from 26 to  $28^\circ\text{C}$  [53]. This process is now ready for the qualification by Airbus. The standard process requires nitric acid deoxidizing prior to PSA treatment. The PSA-treated surface produces an oxide structure of about 1500 nm in thickness with somewhat narrow porous structures in the range from 20 to 25 nm in pore diameter [62]. The PSA process has a reduced process time (in typical, 23 min) and anodizing temperature ( $27^\circ\text{C}$ ), compared with the standard CAA [53]. This leads to an improvement in eco-efficiency by decreasing time and energy consumption and offers a capacity increase.

### 3.3. Lesson learned from serial production of GLARE structures


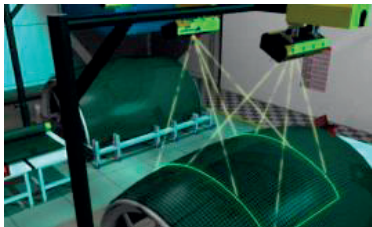
In-process QCs activities are essential if the fits, forms, functions and requirements designed into a part are to be consistently achieved. In general, the QC systems applied to the part production of GLARE structures should be established based on the company's own specifications, part



requirements, engineering drawings. For this purpose, all available QC factors such as pre-scribed contractual requirements, available equipment, level of personnel training and documen-tation systems should be carefully considered. **Table 6** describes the specific lesson learned in part production and the corresponding practical solution.

Issues	Possible practical solutions
<p>Fingerprints or fluid spots on aluminum sheets</p>  <p>[Sealed bags containing prepared rolled aluminum sheets prior to lay-up, source: CompositesWorld]</p>	<ul style="list-style-type: none"><li>• The surface treated aluminum sheets should be stored in dust-free area, or be protected to prevent the further contamination. The sealed bags are typically utilized to protect the bond-primed surfaces of aluminum sheets prior to the lay-up process.</li><li>• Only materials listed in the process specification shall be used in contact with the aluminum sheets inside the net trim line prior to cure. For this purpose, the consumable processing aid materials used in the parts production should be separated into two categories: (1) Contact-use materials: approved for use in direct contact with the anodized (or primed) surface of aluminum sheets. (2) Noncontact-use materials: approved for use as aids to processing but shall not contact the anodized (or primed) aluminum sheets inside the trim line prior to autoclave cure.</li></ul>
<p>Autoclave pressure variations</p>	<ul style="list-style-type: none"><li>• Pressure controller has to regulate the autoclave pressure to maintain a uniform pressure level throughout a cure cycle. In addition, the pressure reservoir shall be kept twice the autoclave pressure so as to operate the pneumatic valves and solenoid valves sufficiently.</li></ul>
<p>Folds and kinks of aluminum sheet</p>  <p>[Roll out over prepreg layers, source: CompositesWorld]</p>	<ul style="list-style-type: none"><li>• During the preparation of thin rolled aluminum sheets (0.2–0.5 mm), consisting of unrolling, cutting, surface treat-ments (i.e. anodizing and bond priming) and conse-quently rolling up, all aluminum sheets should be prepared without folding, or kinks. The damaged material shall not be used for part production. In the stage of lay-up process, the aluminum sheet should be rolled over the un-cured prepreg plies.</li></ul>
<p>Folded prepreg during lay-up process</p>	<ul style="list-style-type: none"><li>• As small regions of prepreg ply are sheared, the surround-ing regions can begin to fold, or wrinkle because of the discontinuity in in-plane strain across the prepreg ply. If the deformation exceeds the limit angle of prepreg material, it is considered to be either fiber wrinkling, or bridging out of the material's tolerance.</li><li>• Pre-cut materials shall be stored in flat, stress-free condi-tion to prevent folding or damage. The damaged material shall not be used for part production.</li></ul>



Issues	Possible practical solutions
<p>Porosities (or voids)</p>  <p>[NDT defect area with air enclosure, source: Fokker]</p>	<ul style="list-style-type: none"> <li>The porosities (or voids) considerably degrade the static strength and fatigue life as a result of insufficient adhesion between aluminum–prepreg and prepreg–prepreg interfaces. Park et al. [6, 35] reported that the reduction in porosity content from 1.30% to 0.69% could account for 46.46% increase in the interlaminar shear strength.</li> <li>High autoclave pressure (in typical. 11 bar) is generally applied to achieve the acceptable porosities (or voids) contents in GLARE parts.</li> </ul>
<p>Prepreg gap controls</p>  <p>[LPS, source: Virtek]</p>	<ul style="list-style-type: none"> <li>The intra-ply gap (i.e. butt-joint) and overlap splices is a common issue in the production of GLARE parts. It is apparent that the manufacturing–induced defects, such as delamination, or fiber missing result in the part thickness variation and the subsequent stress concentrations [63].</li> <li>The requirements of ply collation, such as fiber orientation, location and splice gap are normally specified on the engineering drawing, or corresponding process specification. A LPS with low-intensity laser beams may be utilized for precision controls of ply location, especially on tapered or contoured parts.</li> </ul>
<p>Spring-back after curing process</p>	<ul style="list-style-type: none"> <li>One key challenge in GLARE part production is to fabricate the sound part within tight dimensional tolerances. This issue has been particularly found in the integrated GLARE fuselage panels, for example double curved panels manufactured by SFT process. Orthotropic thermal and chemical properties in combination with autoclave production parameters, such as cure temperature and compaction pressure, are detrimental to achieve this goal.</li> <li>Being able to predict the changes in part configuration allows to design curing tool geometries that already compensate for the undesired change in curvature [64]. This approach can lead to a significant cost reduction for the curing tool-design.</li> </ul>
<p>Disturbed resin squeeze out after curing</p>	<ul style="list-style-type: none"> <li>Insignificant resin bleeding, or squeeze-out in the transverse direction is occasionally observed between two aluminum sheets. This result is attributed to either the loss of vacuum pressure applied consistently, or the absence of curing reaction for epoxy-matrix.</li> <li>At the same time, high compaction pressure is required to compress the materials and squeeze out excess resin.</li> </ul>

**Table 6.** Lesson learned from production of GLARE structures.

## 4. Conclusions

The new hybrid material FML has been successfully applied to the commercial aircraft structures by offering weight savings of 10% compared with conventional aluminum and its alloys, together with benefits that include high tensile strength and better F&DT characteristics and high level of fiber safety. A large number of literatures on the practical applications demonstrates that the material properties of FMLs and their additional interlinked advantages make them the ideal option for thin-walled fuselage shells of next single aisle aircrafts. This chapter dealt with the details of technological developments with ongoing research efforts to understand the material property behaviors of FMLs, especially static strength, F&DT properties and long-term durability. In addition, two prediction methods of MVF and CLT have been introduced to predict the corresponding static properties of FMLs respect to the different lay-up patterns. However, to compete with the typical materials used in aerospace engineering, additional efforts should be directed towards producing consistently sound FML structures at affordable costs and ensuring the stringent quality controls for compliance with structural integrity. Recently, the FML manufacturers have continued to make a substantial progress in production technology, which allows for enabling FMLs in high-volume production rates and increasing affordability for aerospace industry. In addition to the consideration of each constituent material's properties, a strong interfacial bonding between metal sheets and composite layers is one of the key factors for the improvement in joint strength and long-term durability of FML structures. Therefore, a proper surface treatment on the metallic substrate is prerequisite for achieving long-term service capability through more efficient processing in production.

## Author details

Sang Yoon Park<sup>1\*</sup> and Won Jong Choi<sup>2</sup>

\*Address all correspondence to: [hanavia@empas.com](mailto:hanavia@empas.com)

1 Hyundai Automotive Research and Development Division, Hwaseong-Si, Gyeonggi-Do, South Korea

2 Department of Materials Engineering, Korea Aerospace University, Koyang-city, Gyeonggi-Do, South Korea

## References

- [1] Park Y, O'Kelly ME. Examination of cost-efficient aircraft fleets using empirical operation data in US aviation markets. *Journal of Air Transport Management*. 2018;**69**:224-234. DOI: 10.1016/j.jairtraman.2017.02.002

- [2] Alderliesten RC, Homan J. Fatigue and damage tolerance issues of GLARE in aircraft structures. *International Journal of Fatigue*. 2006;**28**:1116-1123. DOI: 10.1016/j.ijfatigue.2006.02.015
- [3] Fontain L. NDT on A380. In: 48th Annual Non-Destructive Testing (NDT) Forum; 20–22 September 2005; Orlando, Florida
- [4] Beumler T. Fiber metal laminate structures—From laboratory to application. In: Invitation to an RAeS Lecture in Cooperation with the DGLR and VDI (Presented to the Royal Aerospace Society Hamburg Branch at Hamburg University of Applied Science); 29th October 2009; Hamburg, Germany
- [5] Roebroeks GHJJ. Glare features. In: Vlot A, Gunnink JW, editors. *Fibre Metal Laminates: An Introduction*. The Netherlands: Kluwer Academic Publishers; 2001. pp. 23-37. DOI: 10.1007/978-94-010-0995-9\_2
- [6] Park SY, Choi WJ, Choi HS, Kwon H. Effects of surface pre-treatment and void content on GLARE laminate process characteristics. *Journal of Materials Processing Technology*. 2010;**210**:1008-1016. DOI: 10.1016/j.jmatprotec.2010.01.017
- [7] Subbaramaiah R, Prusty BG, Pearce GMK, Lim SH, Thomson RS. Crashworthy response of fibre metal laminate top hat structures. *Composite Structures*. 2017;**160**:773-781. DOI: 10.1016/j.compstruct.2016.10.112
- [8] Botelho EC, Almeida RS, Pardini LC, Rezende MC. Elastic properties of hygrothermally conditioned GLARE laminate. *International Journal of Engineering Science*. 2007;**45**: 163-172. DOI: 10.1016/j.ijengsci.2006.08.017
- [9] Shim DJ, Alderliesten RC, Spearing SM, Burianek DA. Fatigue crack growth prediction in GLARE hybrid laminates. *Composites Science and Technology*. 2003;**63**:1759-1767. DOI: 10.1016/S0266-3538(03)00082-4
- [10] Müller B, Hagenbeek M, Sinke J. Thermal cycling of (heated) fibre metal laminates. *Composite Structures*. 2016;**152**:106-116. DOI: 10.1016/j.compstruct.2016.05.020
- [11] Sinmazçelik T, Avcu E, Özgür Bora M, Çoban O. A review: Fibre metal laminates, background, bonding types and applied test methods. *Materials & Design*. 2011;**32**:3671-3685. DOI: 10.1016/j.matdes.2011.03.011
- [12] Rans CD. Bolted joints in glass reinforced aluminium (GLARE) and other hybrid fibre metal laminates (FML). In: Camanho P, Tong L, editors. *Composite Joints and Connections: Principles, Modelling and Testing*. Oxford: Woodhead Publishing Limited; 2011. pp. 35-76. DOI: 10.1533/9780857094926.1.35
- [13] Assler H, Telgkamp J. Design of aircraft structures under special consideration of NDT. In: 9th European Conference on NDT; 25–29 September 2006; Berlin, Germany
- [14] Asundi A, Choi AYN. Fiber metal laminates: An advanced material for future aircraft. *Journal of Materials Processing Technology*. 1997;**63**:384-394. DOI: 10.1016/S0924-0136(96)02652-0

- [15] Vogelesang LB, Vlot A. Development of fibre metal laminates for advanced. *Journal of Materials. Processing Technology*. 2000;**103**:1-5. DOI: 10.1016/S0924-0136(00)00411-8
- [16] Ye L, Lu Y, Su Z, Meng G. Functionalized composite structures for new generation airframes: A review. *Composites Science and Technology*. 2005;**65**:1436-1446. DOI: 10.1016/j.compscitech.2004.12.015
- [17] Schut J, Alderliesten RC. Delamination growth rate at low and elevated temperatures in GLARE. In: 25th International Congress of the Aeronautical Sciences; 3-8 September 2006; Hamburg, Germany. pp. 1-7
- [18] Botelho EC, Silva RA, Pardini LC, Rezende MC. A review on the development and properties of continuous fiber/epoxy/aluminum hybrid composites for aircraft structures. *Materials Research*. 2006;**9**:247-256. DOI: 10.1590/S1516-14392006000300002
- [19] Hamill L, Hofmann DC, Nutt S. Galvanic corrosion and mechanical behavior of fiber metal laminates of metallic glass and carbon fiber composites. *Advanced Engineering Materials*. 2017;**20**:1700-1711. DOI: 10.1002/adem.201700711
- [20] Wang WX, Takao Y, Matsubara T. Galvanic corrosion-resistant carbon fiber metal laminates. In: 16th International Conference on Composite Materials; 8–13 July 2007; Kyoto, Japan. pp. 1-10
- [21] Pan Y, Wu X, Zh H, Wu G, Sun S, Ye H, Zhang Z. A new approach to enhancing interlaminar strength and galvanic corrosion resistance of CFRP/Mg laminates. *Composites Part A: Applied Science and Manufacturing*. 2018;**105**:78-86. DOI: 10.1016/j.compositesa.2017.11.009
- [22] Vlot A, Vogelesang LB, de Vries TJ. Towards application of fibre metal laminates in large aircraft. *Aircraft Engineering and Aerospace Technology*. 1999;**71**:558-570. DOI: 10.1108/00022669910303711
- [23] Wittenberg TC, van Baten TJ, de Boer A. Design of fiber metal laminate shear panels for ultra-high capacity aircraft. *Aircraft Design*. 2001;**4**:99-113. DOI: 10.1016/S1369-8869(01)00003-9
- [24] Along the Bond Line—Groundbreaking Aircraft Structures [Internet]. Available from: ([http://www.fokker.com/sites/default/files/media/Files/Brochures/Fokker\\_Glare.pdf](http://www.fokker.com/sites/default/files/media/Files/Brochures/Fokker_Glare.pdf)) [Accessed: April 14, 2018]
- [25] Campilho RDSG, da Silva LFM, Banea MD. Adhesive bonding of polymer composites to lightweight metals. In: Amancio-Filho ST, Blaga LA, editors. *Joining of Polymer-Metal Hybrid Structures: Principles and Applications*. New York: John Wiley & Sons, Inc; 2017. pp. 29-59. DOI: 10.1002/9781119429807.ch2
- [26] Wu G, Yang JM. The mechanical behavior of GLARE laminates for aircraft structures. *The Journal of the Minerals, Metals & Materials Society*. 2005;**57**:72-79. DOI: 10.1007/s11837-005-0067-4

- [27] Spronk SWF, Şen I, Alderliesten RC. Predicting fatigue crack initiation in fibre metal laminates based on metal fatigue test data. *International Journal of Fatigue*. 2015;**70**:428-439. DOI: 10.1016/j.ijfatigue.2014.07.004
- [28] Vogelesang LB, Schijve J, Fredell R. Fibre-metal laminates: Damage tolerant aerospace materials. In: Demaid A, de Wit JHW, editors. *Case Studies in Manufacturing with Advanced Materials*, Vol. 2. Amsterdam: Elsevier; 1995. pp. 253-271. DOI: 10.1016/0925-8388(96)80048-X
- [29] Hagenbeek M, van Hengel C, Bosker OJ, Vermeeren CAJR. Static properties of fibre metal laminates. *Applied Composite Materials*. 2003;**10**:207-222. DOI: 10.1023/A:1025569316827
- [30] Vogelesang B, Gunnink JW, Roebroeks GHJJ, Muè Ller RPG. Toward the supportable and durable aircraft fuselage structure. In: *Proceedings of the 18th Symposium of the International Committee on Aeronautical Fatigue*; 3-5 May 1995; Melbourne, Australia. pp. 257-272
- [31] Cortes P, Cantwell WJ. The prediction of tensile failure in titanium-based thermoplastic fibre-metal laminates. *Composites Science and Technology*. 2006;**66**:2306-2316. DOI: 10.1016/j.compscitech.2005.11.031
- [32] Cortés P, Cantwell WJ. Fracture properties of a fiber-metal laminates based on magnesium alloy. *Journal of Materials Science* 2004;**39**:1081-1083. DOI: 10.1016/j.compositesb.2005.06.002
- [33] Alderliesten RC, Hagenbeek M, Homan JJ, Hooijmeijer PA, de Vries TJ, Vermeeren CAJR. Fatigue and damage tolerance of GLARE. *Applied Composite Materials*. 2003;**10**:223-242. DOI: 10.1023/A:1025537818644
- [34] Hooijmeijer PA. Burn-through and lightning strike. In: Vlot A, Gunnink JW, editors. *Fibre Metal Laminates: An Introduction*. The Netherlands: Kluwer Academic Publishers; 2001. pp. 399-408. DOI: 10.1007/978-94-010-0995-9\_26
- [35] Park SY, Choi WJ, Choi HS. The effects of void contents on the long-term hygrothermal behaviors of glass/epoxy and GLARE laminates. *Composite Structures*. 2010;**92**:18-24. DOI: 10.1016/j.compstruct.2009.06.006
- [36] Remmers JJC, de Borst R. Delamination buckling of fibre-metal laminates. *Composites Science and Technology*. 2001;**61**:2207-2213. DOI: 10.1016/S0266-3538(01)00114-2
- [37] Frizzell RM, McCarthy CT, McCarthy MA. A comparative study of the pin-bearing responses of two glass-based fibre metal laminates. *Composites Science and Technology*. 2008;**68**:3314-3321. DOI: 10.1016/j.compscitech.2008.08.021
- [38] Şen I, Alderliesten RC, Benedictus R. Lay-up optimisation of fibre metal laminates based on fatigue crack propagation and residual strength. *Composite Structures*. 2015;**124**:77-87. DOI: 10.1016/j.compstruct.2014.12.060
- [39] Sadighi M, Alderliesten RC, Benedictus R. Impact resistance of fiber-metal laminates: A review. *International Journal of Impact Engineering*. 2012;**49**:77-90. DOI: 10.1016/j.ijimpeng.2012.05.006



- [40] Wischmann G. In: Wissenschaftliches Festkolloquium; 2006. Available online at [www.iff.uni-stuttgart.de](http://www.iff.uni-stuttgart.de)
- [41] Airbus Customers Benefit from Fiber Metal Laminates [Internet]. Available from: (<https://www.scribd.com/document/35637377/ILA06-Praesentat-AIRBUS-Juergen-Pleitner>) [Accessed: April 14, 2018]
- [42] Muchiri AK. Maintenance Planning Optimisation for the Boeing 737 Next Generation [Thesis]. Delft, The Netherlands: Delft University of Technology; 2002
- [43] Rans C, Morinière F, Rodi R, Alderliesten R, Benedictus R. Fatigue behavior of fiber/metal laminate panels containing internal carbon tear straps. *Journal of Aircraft*. 2011;**48**:2122-2129. DOI: 10.2514/1.C031475
- [44] Beumler T. Flying GLARE [Thesis]. Delft, The Netherlands: Delft University of Technology; 2004
- [45] Alderliesten R, Rans C, Benedictus R. The applicability of magnesium based fibre metal laminates in aerospace structures. *Composites Science and Technology* 2008;**68**:2983-2993. DOI: 10.1016/j.compscitech.2008.06.017
- [46] Park SY, Choi WJ, Choi HS, Kwon H, Kim SH. Recent trends in surface treatment technologies for airframe adhesive bonding processing: A review (1995–2008). *The Journal of Adhesion*. 2010;**86**:192-221. DOI: 10.1080/00218460903418345
- [47] Zhang X, Ma Q, Dai Y, Hu F, Liu G, Xu Z, Wei G, Xu T, Zeng Q, Xie W. Effects of surface treatments and bonding types on the interfacial behavior of fiber metal laminate based on magnesium alloy. *Applied Surface Science*. 2018;**427**:897-906. DOI: 10.1016/j.apsusc.2017.09.024
- [48] Li X, Zhang X, Zhang H, Yang JL, Nia AB, Chai GB. Mechanical behaviors of Ti/CFRP/Ti laminates with different surface treatments of titanium sheets. *Composite Structures*. 2017;**163**:21-31. DOI: 10.1016/j.compstruct.2016.12.033
- [49] Pan YC, Wu GQ, Huang Z, Li MY, Ji SD, Zhang ZK. Effects of surface pre-treatments on mode I and mode II interlaminar strength of CFRP/Mg laminates. *Surface and Coatings Technology*. 2017;**319**:309-317. DOI: 10.1016/j.surfcoat.2017.04.010
- [50] Aghamohammadi H, Abbandanak SNH, Eslami-Farsani R, Siadati SMH. Effects of various aluminum surface treatments on the basalt fiber metal laminates interlaminar adhesion. *International Journal of Adhesion and Adhesives*. 2018;**84**:184-193. DOI: 10.1016/j.ijadhadh.2018.03.005
- [51] Critchlow GW, Yendall KA, Bahrani D, Quinn A, Andrews F. Strategies for the replacement of chromic acid anodising for the structural bonding of aluminium alloys. *International Journal of Adhesion and Adhesives*. 2006;**26**:419-453. DOI: 10.1016/j.ijadhadh.2005.07.001
- [52] Bjørgum A, Lapique F, Walmsley J, Redford K. Anodising as pre-treatment for structural bonding. *International Journal of Adhesion and Adhesives*. 2003;**23**:401-412. DOI: 10.1016/S0143-7496(03)00071-X

- [53] Matz CW, Hilling B, Kelm W, Kock E. Phosphoric Sulfuric Acid Anodizing (PSA) – A Heavy Metal Free Alternative for High Quality Surface Pretreatment of Aluminum. In: 83rd Meeting of the AGARD Structures and Materials Panel; 4–5 September 1996; Florence, Italy
- [54] Oosting R. Toward a New Durable and Environmentally Compliant Adhesive Bonding Process for Aluminum Alloys [Thesis]. Delft, The Netherlands: Delft University of Technology; 1995
- [55] Brockmann W, Hennemann OD, Kollek H. Surface properties and adhesion in bonding aluminium alloys by adhesives. *International Journal of Adhesion and Adhesives*. 1982;2: 33-40. DOI: 10.1016/0143-7496(82)90064-1
- [56] Smith T, Lindberg G. Surface tools for automated non-destructive inspection of contamination. *Surface Technology*. 1979;9:1-29. DOI: 10.1016/0376-4583(79)90080-3
- [57] Everett RA, Johnson WS. Repeatability of mixed-mode adhesive debonding. In: Johnson WS, editors. *Delamination and Debonding of Materials*. Philadelphia: ASTM International; 1983. pp. 267-281. DOI: 10.1520/STP36309S
- [58] Venables JD. Adhesion and durability of metal-polymer bonds. *Journal of Materials Science*. 1984;19:2431-2453. DOI: 10.1007/BF00550796
- [59] Bishopp J. Surface pretreatment for structural bonding. In: Cognard P, editor. *Handbook of Adhesives and Sealants*. Vol. 1. Amsterdam: Elsevier; 2005. pp. 163-214. DOI: 10.1016/S1874-5695(02)80005-7
- [60] Zhang JS, Zhao XH, Zuo Y, Xiong JP. The bonding strength and corrosion resistance of aluminum alloy by anodizing treatment in a phosphoric acid modified boric acid/sulfuric acid bath. *Surface and Coatings Technology*. 2008;202:3149-3156. DOI: 10.1016/j.surfcoat.2007.10.041
- [61] Domingues L, Fernandes JCS, Cunha Belo MD, Ferreira MGS, Guerra-Rosa L. Anodising of Al 2024-T3 in a modified sulphuric acid/boric acid bath for aeronautical applications. *Corrosion Science*. 2003;45:149-160. DOI: 10.1016/S0010-938X(02)00082-3
- [62] Velterop L. Phosphoric Sulphuric Acid Anodising: An Alternative for Chromic Acid Anodising in Aerospace Applications. Amsterdam, The Netherlands: National Aerospace Laboratory (NLR). Report number: NLR-TP-2003–210; 2003
- [63] Nardi D, Abouhamzeh M, Leonard R, Sinke J. Detection and evaluation of prepreg gaps and overlaps in GLARE laminates. *Applied Composite Materials*. DOI: 10.1007/s10443-018-9679-z
- [64] Abouhamzeh M, Sinke J, Benedictus R. Investigation of curing effects on distortion of fibre metal laminates. *Composite Structures*. 2015;122:546-552. DOI: 10.1016/j.compstruct.2014.12.019